# REPORT DOCUMENTATION PAGE

Form Approved OMB NO. 0704-0188



| 1. REPORT DATE (DD-MM-YYYY) | 2. REPORT TYPE | 3. DATES COVERED (From - To) |
|---|---|---|
| 18-04-2016 | Final Report | 1-Feb-2015 - 31-Jan-2016 |

**4. TITLE AND SUBTITLE**
Final Report: Raman Spectrometer for the Characterization of Advanced Materials and Nanomaterials

**5a. CONTRACT NUMBER**
W911NF-15-1-0063

**5b. GRANT NUMBER**

**5c. PROGRAM ELEMENT NUMBER**
106012

**6. AUTHORS**
Dorina Chipara

**5d. PROJECT NUMBER**

**5e. TASK NUMBER**

**5f. WORK UNIT NUMBER**

**7. PERFORMING ORGANIZATION NAMES AND ADDRESSES**
University of Texas-Rio Grande Valley
1201 W. University Drive

Edinburg, TX 78539 -2909

**8. PERFORMING ORGANIZATION REPORT NUMBER**

**9. SPONSORING/MONITORING AGENCY NAME(S) AND ADDRESS (ES)**
U.S. Army Research Office
P.O. Box 12211
Research Triangle Park, NC 27709-2211

**10. SPONSOR/MONITOR'S ACRONYM(S)**
ARO

**11. SPONSOR/MONITOR'S REPORT NUMBER(S)**
66369-MS-REP.1

**12. DISTRIBUTION AVAILIBILITY STATEMENT**
Approved for Public Release; Distribution Unlimited

**13. SUPPLEMENTARY NOTES**
The views, opinions and/or findings contained in this report are those of the author(s) and should not contrued as an official Department of the Army position, policy or decision, unless so designated by other documentation.

**14. ABSTRACT**
The grant focused on the purchase of a Renishaw InVia Raman microscope to support and enhance the research in nanomaterials at The University of Texas Rio Grande Valley. The system was purchased, according to the description provided in the proposal (two laser beam capabilities at 785 nm and 532 nm, cell for temperature dependence capabilities manufactured by Linkam, and filters for low wave numbers for the 785 nm laser. The system includes an accessory for polarization (for 785 nm) and an optical cable that allows external Raman measurements. The manufacturer installed the system and provided the training of the main users. The Users

**15. SUBJECT TERMS**
Raman Spectrometer, measurements

| 16. SECURITY CLASSIFICATION OF: | | | 17. LIMITATION OF ABSTRACT | 15. NUMBER OF PAGES | 19a. NAME OF RESPONSIBLE PERSON |
|---|---|---|---|---|---|
| a. REPORT | b. ABSTRACT | c. THIS PAGE | | | Dorina Chipara |
| UU | UU | UU | UU | | 19b. TELEPHONE NUMBER 956-665-3521 |

**Report Title**

Final Report: Raman Spectrometer for the Characterization of Advanced Materials and Nanomaterials

**ABSTRACT**

The grant focused on the purchase of a Renishaw InVia Raman microscope to support and enhance the research in nanomaterials at The University of Texas Rio Grande Valley. The system was purchased, according to the description provided in the proposal (two laser beam capabilities at 785 nm and 532 nm, cell for temperature dependence capabilities manufactured by Linkam, and filters for low wave numbers for the 785 nm laser. The system includes an accessory for polarization (for 785 nm) and an optical cable that allows external Raman measurements. The manufacturer installed the system and provided the training of the main users. The Users confirmed that the system fulfills the technical requirements. Preliminary data have been obtained and undergraduate/graduate students started their research by using this Raman Spectrometer.

---

## Enter List of papers submitted or published that acknowledge ARO support from the start of the project to the date of this printing. List the papers, including journal references, in the following categories:

### (a) Papers published in peer-reviewed journals (N/A for none)

Received Paper

**TOTAL:**

**Number of Papers published in peer-reviewed journals:**

---

### (b) Papers published in non-peer-reviewed journals (N/A for none)

Received Paper

**TOTAL:**

**Number of Papers published in non peer-reviewed journals:**

---

## (c) Presentations

American Physical Society

1. Omar Espino, Brian Yust, Dorina Chipara, Pullickel Ajayan, Alin Chipara, Mircea Chipara. Microwave Irradiation on Halloysite - Polypropylene Nanocomposites. T1.00139, Poster Session III, Thursday, 1:00 pm - 4:00 pm, March 17, 2016, APS March Meeting 2016, Monday-Friday, March 14-18, 2016; Baltimore, Maryland, USA.

2. Fernando Flor, Pullickel Ajayan, Alin Chipara, Karen Lozano, Dorina Chipara, Robert Vajtai, Mircea Chipara. On the Radial Breathing Mode in SWCNTs dispersed within PVC. T1.00140 Poster Session III. Thursday, 1:00 pm - 4:00 pm, March 17, 2016, APS March Meeting 2016, Monday-Friday, March 14-18, 2016, Baltimore, Maryland, USA.

3. Filipe Ferreira, Felipe Brito, Dorina Chipara, Pullickel Ajayan, Wesley Francisco, Cristian Chipara, Evelyn Simonetti, Charles Cartwright, Luciana Cividanes, James Hinthorne, Gilmar Thim, Robert Vajtai, Mircea Chipara. Spectroscopic Studies on Graphenes Dispersed Within Polymeric Matrices T1.00068. Poster Session III. Thursday, 1:00 pm - 4:00 pm, March 17, 2016, APS March Meeting 2016, Monday-Friday, March 14-18, 2016; Baltimore, Maryland, USA.

4. Julio Cantu, Cristian Chipara, Pullickel Ajayan, James Hinthorne, Mircea Chipara. Raman Investigations of PVDF-BaTiO3 Nanocomposites. E42.00011, Session E42: Bi-Component Systems: Composites and Blends, Tuesday, 10:24 AM–10:36 AM, March 15, 2016, Room: 345 APS March Meeting 2016, Baltimore, Maryland, USA.

5. Arnold Fonseca, Dorina Chipara, Karen Lozano, Mircea Chipara. Wide Angle X-Ray Scattering Investigations on Irradiated iPP-VGCNF Nanocomposites. M1.00091. Session M1: Poster Session II, 11:30 am - 2:30 pm, Wednesday March 16, 2016. APS March Meeting 2016, Baltimore, Maryland, USA.

6. Roberto Rangel, Dorina Chipara, Brian Yust, Desiree Padilla, Mircea Chipara. Water - Based TiO2 Suspensions: A Raman Study. M1. 00280. Session M1: Poster Session II, Wednesday 11:30 am - 2:30 pm, March 16, 2016. APS March Meeting 2016, Baltimore, Maryland, USA

7. Andres Salgado, Robert Jones, Samantha Ramirez, Ibrahim Elamin, James Hinthorne, Mircea Chipara. PVC-OH Functionalized SWCNT Nanocomposites. Session E42: Bi-Component Systems: Composites and Blends Room: 345. E42.000089:48 AM–10:00 AM Tuesday, March 15, 2016. APS March Meeting 2016, Baltimore, Maryland, USA.

8. Oscar Guerrero, Samantha Ramirez, Robert Jones, Brian Yust, James Hinthorne, Mircea Chipara. Spectroscopic Investigations on PVDF-MWCNTs. S42.00012. Session S42: Assembly of Nanoparticles Nanocomposites 11:15 AM–2:15 PM, Thursday, March 17, 2016 Room: 345, APS March Meeting 2016, Baltimore, Maryland, USA.

9. Jorge Cisneros, Brian Yust, Mircea Chipara Microwave Irradiation on Graphene Dispersed Within Polymeric Matrices M1.00106 Session M1: Poster Session II, Wednesday, 11:30 am - 2:30 pm. APS March Meeting 2016, Baltimore, Maryland, USA.

American Chemical Society Spring Meeting.

10. Mircea Chipara, Elamin Ibrahim, Dorina M. Chipara, Julian A. Martinez, Raman investigations on nanocomposites of colloidal silver in block copolymers. Contribution presented to the 251st American Chemical Society Spring Meeting, DIVISION: POLY 405 SYMPOSIUM Responsive Nanostructures & Nanocomposites, San Diego, 13-17 March, 2016.

(d) Manuscripts submitted for publication in peer reviewed journals:

1. Yunlong Jin, Shah Valloppilly, Dorina Magdalena Chipara, Ralph Skomski, Mircea Chipara*, Wenyong Zhang, Maximilian Villarreal, David J. Sellmyer, On Polystyrene - Block Polyisoprene – Block Polystyrene Filled with C Coated Ni Nanoparticles, Journal of Materials Science, submitted.

**Number of Presentations:** 11.00

## Non Peer-Reviewed Conference Proceeding publications (other than abstracts):

Received Paper

**TOTAL:**

**Number of Non Peer-Reviewed Conference Proceeding publications (other than abstracts):**

## Peer-Reviewed Conference Proceeding publications (other than abstracts):

Received Paper

**TOTAL:**

**Number of Peer-Reviewed Conference Proceeding publications (other than abstracts):**

## (d) Manuscripts

Received Paper

**TOTAL:**

**Number of Manuscripts:**

## Books

Received Book

**TOTAL:**

Received Book Chapter

**TOTAL:**

## Patents Submitted

## Patents Awarded

## Awards

## Graduate Students

| NAME | PERCENT_SUPPORTED | Discipline |
|---|---|---|
| Maximllian Villarreal | 0.00 | |
| **FTE Equivalent:** | **0.00** | |
| **Total Number:** | **1** | |

## Names of Post Doctorates

| NAME | PERCENT_SUPPORTED |
|---|---|
| **FTE Equivalent:** | |
| **Total Number:** | |

## Names of Faculty Supported

| NAME | PERCENT_SUPPORTED | National Academy Member |
|---|---|---|
| Dorina Chipara | 0.00 | |
| Mircea Chipara | 0.00 | |
| Brian Yust | 0.00 | |
| Elamin Ibrahim | 0.00 | |
| Louis Materon | 0.00 | |
| **FTE Equivalent:** | **0.00** | |
| **Total Number:** | **5** | |

## Names of Under Graduate students supported

| NAME | PERCENT_SUPPORTED | Discipline |
|---|---|---|
| Julian A. Martinez | 0.00 | Chemistry |
| Omar Espino | 0.00 | Physics |
| Fernando Flor | 0.00 | Physics |
| Julio Cantu | 0.00 | Physics |
| Arnold Fonseca | 0.00 | Physics |
| Robert Rangel | 0.00 | Physics |
| Andres Salgado | 0.00 | Physics |
| Oscar Guerrero | 0.00 | Physics |
| Jorge Cisneros | 0.00 | Physics |
| Andres Marroquin | 0.00 | Mechanical Engineering |
| Suzana Campos | 0.00 | Mechanical Engieering |
| **FTE Equivalent:** | **0.00** | |
| **Total Number:** | **11** | |

## Student Metrics

This section only applies to graduating undergraduates supported by this agreement in this reporting period

The number of undergraduates funded by this agreement who graduated during this period: ..... 0.00

The number of undergraduates funded by this agreement who graduated during this period with a degree in science, mathematics, engineering, or technology fields:..... 0.00

The number of undergraduates funded by your agreement who graduated during this period and will continue to pursue a graduate or Ph.D. degree in science, mathematics, engineering, or technology fields:..... 0.00

Number of graduating undergraduates who achieved a 3.5 GPA to 4.0 (4.0 max scale):..... 0.00

Number of graduating undergraduates funded by a DoD funded Center of Excellence grant for Education, Research and Engineering:..... 0.00

The number of undergraduates funded by your agreement who graduated during this period and intend to work for the Department of Defense ..... 0.00

The number of undergraduates funded by your agreement who graduated during this period and will receive scholarships or fellowships for further studies in science, mathematics, engineering or technology fields: ..... 0.00

## Names of Personnel receiving masters degrees

| NAME |
|---|
| **Total Number:** |

## Names of personnel receiving PHDs

NAME

**Total Number:**

## Names of other research staff

NAME PERCENT_SUPPORTED

**FTE Equivalent:**
**Total Number:**

## Sub Contractors (DD882)

## Inventions (DD882)

## Scientific Progress

See Attachment

## Technology Transfer

The following research directions were ignited by the acquisition of the Renishaw InVia Raman Confocal Microscope:

**Semiconducting Nanoparticles for Future Biological and Medical Applications**

This preliminary research focused on $TiO_2$ nanoparticles. These nanoparticles have been considered for the following reasons: 1). Relatively small $TiO_2$ nanoparticles (average size below 50 nm) are available from many vendors at a relatively low price. 2). $TiO_2$ is a semiconducting material. 3). The role of $TiO_2$ in the generation of reactive oxygen species in the presence of water and electromagnetic radiation is well documented. 4. The antibacterial features are still under debate.

Our point of view is that $TiO_2$ has antibacterial features solely if UV radiation (or component) is present. Dark properties of $TiO_2$ may not include antibacterial features. Fig. 1 shows the typical Raman spectrum of $TiO_2$ (anatase) at various powers and the assignment for each line. Spectrum has been recorded by using the 785 nm incident laser beam.

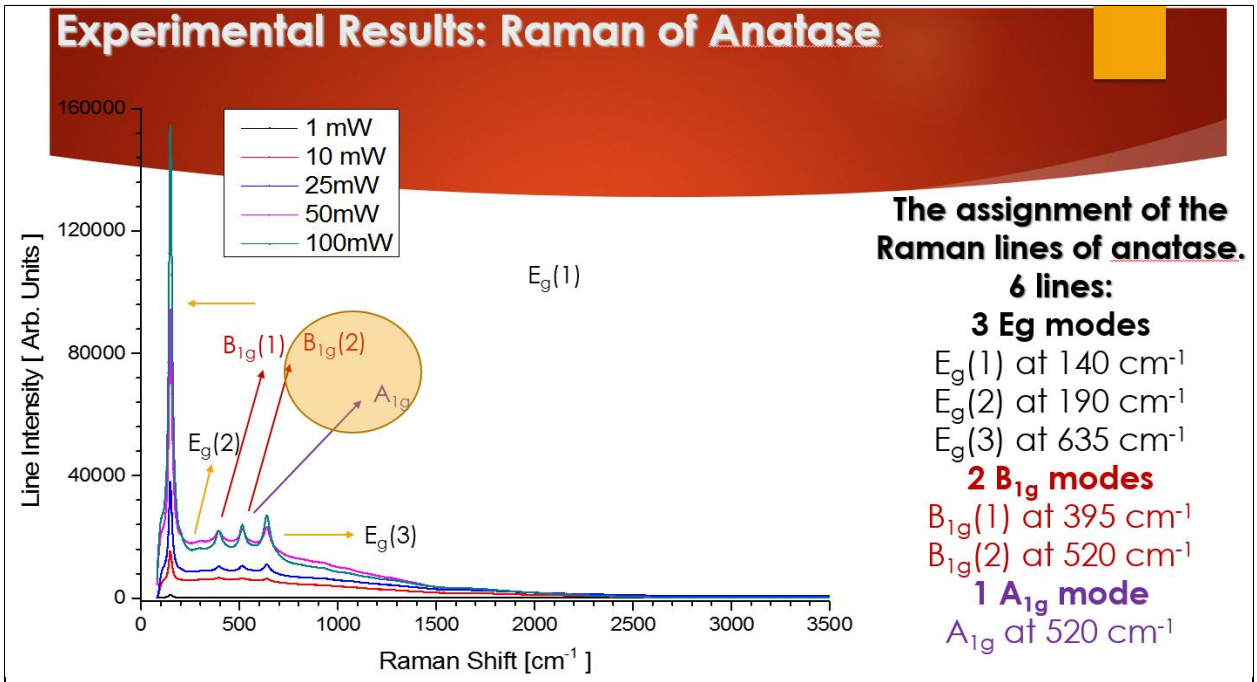


*Figure 1. Raman spectrum of TiO2 powder*

Dispersions of $TiO_2$ into a polymeric matrix (Polyethylene oxide; PEO) have been prepared by solution method dissolving the polymer matrix in deionized water, mixing the solution with various amounts of

$TiO_2$, sonicating the mixture 30 minutes for a good dispersion of the nanofiller and removing the residual solvent by heating in an oven at 90 $^oC$.

The Raman spectrum of PEO-TiO2 is shown in Fig. 2. It is easily noticed that the Raman lines of $TiO_2$ dominates the wavelength ranging from 100 up to about 800 $cm^{-1}$, where the polymer has some weak lines. This study indicated that the Raman spectrometer can detect quantities containing as low as 1% wt. $TiO_2$ and indicated that the best line to focus on is the line located at about 125 $cm^{-1}$. This line, which is the most intense component of the Raman spectrum of $TiO_2$, is typically intense and narrow.

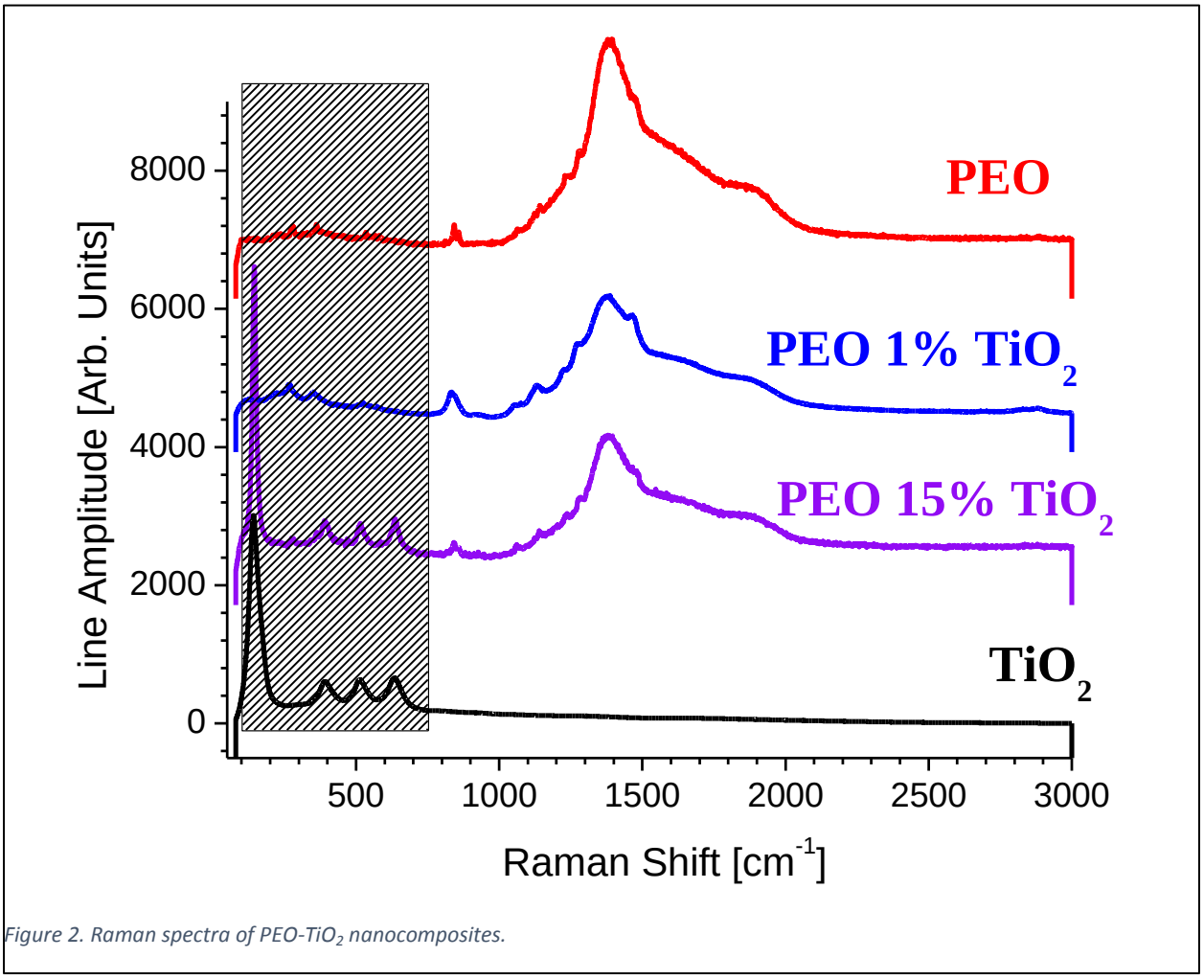


*Figure 2. Raman spectra of PEO-$TiO_2$ nanocomposites.*

However, a shift of the Raman line, connected to the size of $TiO_2$ nanoparticles was noticed. The shift may indicate also a change in the phase composition although Wide Angle X-Ray Scattering was not able to support such hypothesis.

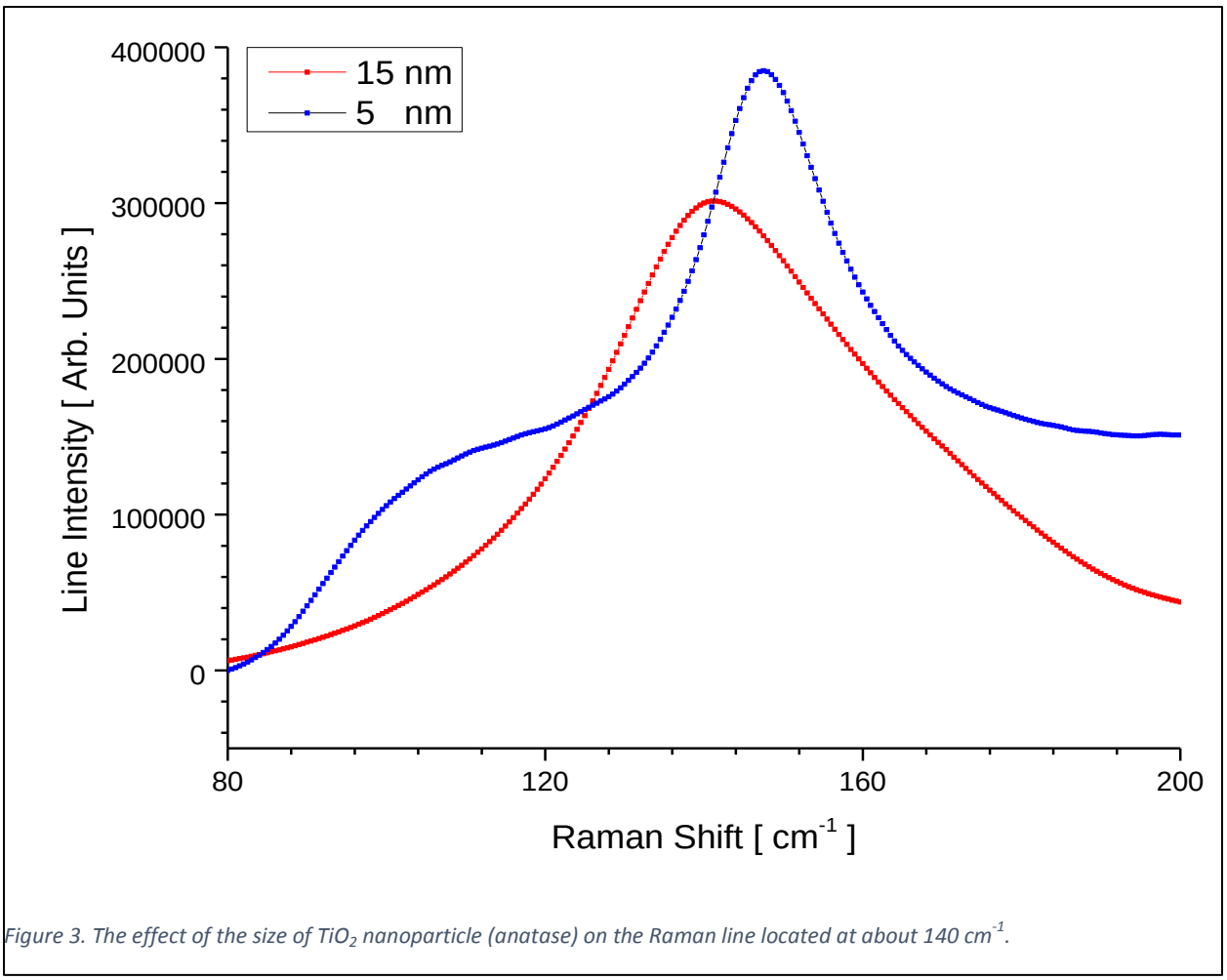


*Figure 3. The effect of the size of $TiO_2$ nanoparticle (anatase) on the Raman line located at about 140 $cm^{-1}$.*

Dispersions of $TiO_2$-deionized water and $TiO_2$-nutrients have been prepared. The recording of the Raman spectra was difficult as the focal point for light did not coincides to the optical point for the Raman laser. However, we have exploited the z scanning capability to obtain the Raman spectra of sediment $TiO_2$ nanoparticles. It was confirmed that the spectral region between 100 and 200 $cm^{-1}$ is not affected by the presence of water or nutrients. Next steps will include the study of $TiO_2$-nutrients-bacteria systems and the development of the accessories for dark and light investigations.

This topic was the central point of an undergraduate senior thesis (student Desiree Padilla) and of a poster presentation at APS 2016.

**Raman Investigations on carbon nanostructures dispersed within polymeric matrices.**

PS-PI-PS-Graphene nanocomposites. Polystyrene-block polyisoprene - block polystyrene three block copolymer purchased from Sigma Aldrich has been loaded with graphene nanoparticles purchased from CheapTubes Inc., by using the solution method, with chloroform as solvent. The preliminary results were

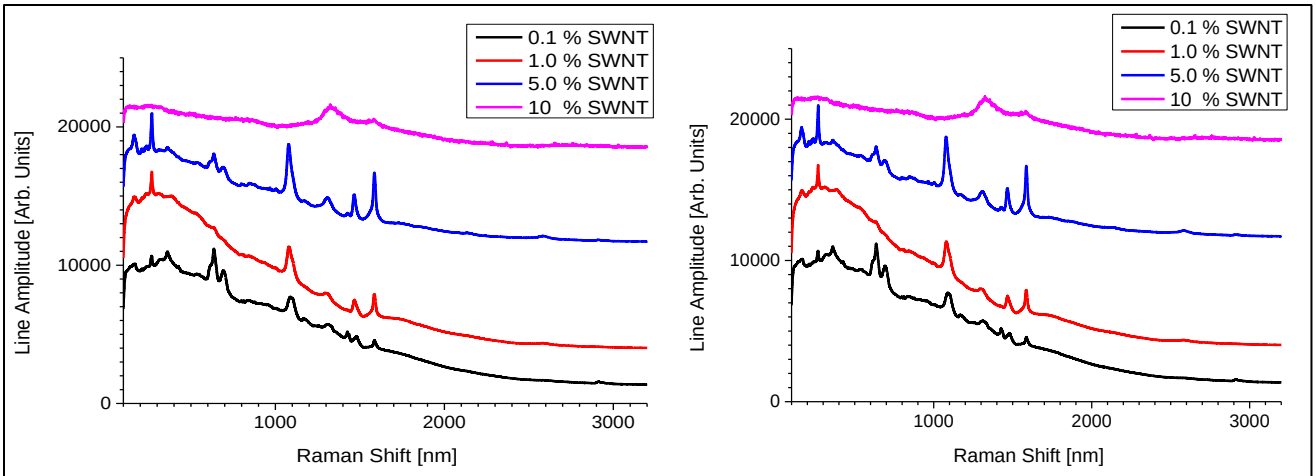


*Figure 5 Raman spectra of PVC filled with SWNT-OH*

included in the poster **Microwave Irradiation on Graphene Dispersed Within Polymeric Matrices** by authors Jorge Cisneros, Brian Yust, Mircea Chipara, where Jorge Cisneros is an undergraduate student. Another research aimed at OH functionalized single walled carbon nanotubes dispersed within polyvinylchlorine (presented at the APS March meeting 2016) as **PVC-OH Functionalized SWCNT Nanocomposites by authors** Andres Salgado, Robert Jones, Samantha Ramirez, Ibrahim Elamin, James Hinthorne, Mircea Chipara.

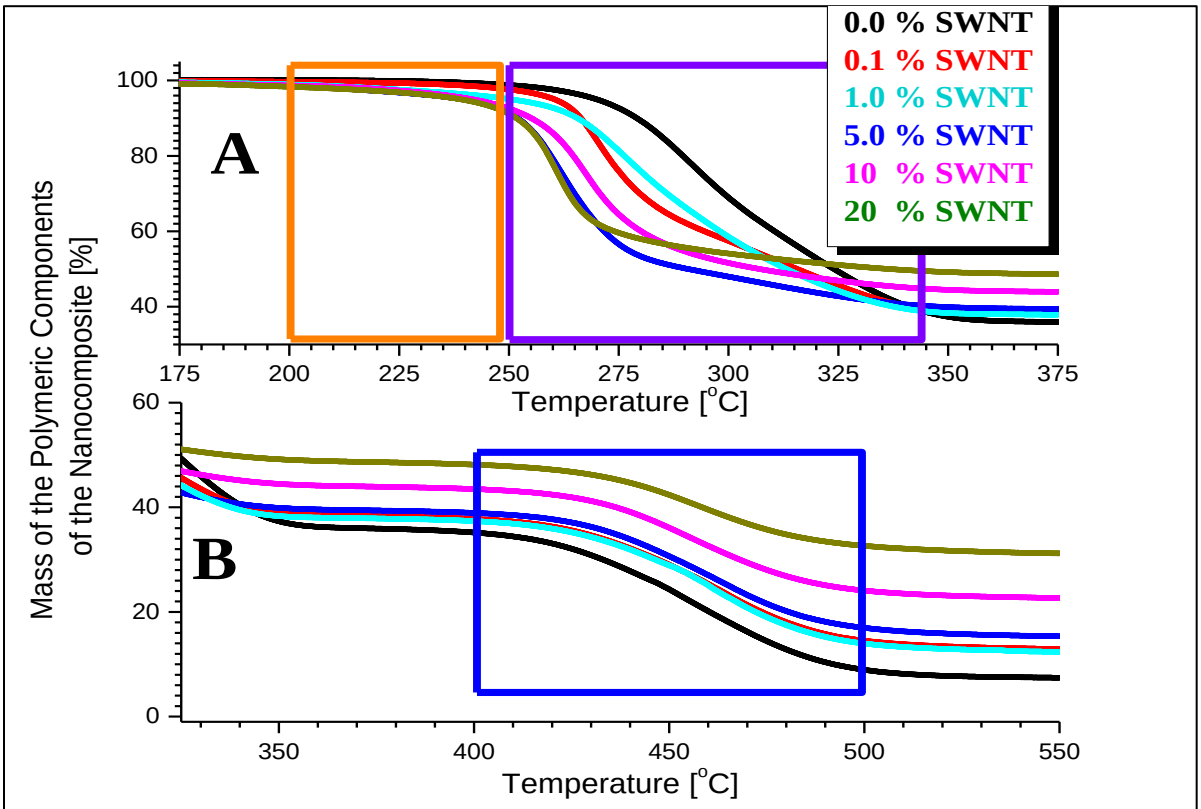


*Figure 4. Thermal degradation of PVC-SWNT-OH nanocomposites in nitrogen atmosphere. TGA data.*

The Raman spectra at room temperature is shown in Fig. 4. We are focusing now at the effect of temperature on the Raman spectra. According to TGA, the polymer exhibits a two steps degradation in nitrogen (see Fig. 5) and oxygen atmosphere.

Additional information about preliminary results and experiments is included in the list of publications. During this period, a single manuscript has been submitted for publication to Journal of Materials Science (Springer).

# On Polystyrene - Block Polyisoprene – Block Polystyrene Filled with C Coated Ni Nanoparticles

Yunlong Jin[1], Shah Valloppilly[1], Dorina Magdalena Chipara[2], Ralph Skomski[1], Maximiliano Villarreal[2], Mircea Chipara[2*], Wenyong Zhang[1], David J. Sellmyer[1]

[1]The University of Nebraska, Nebraska Center for Materials and Nanoscience, Lincoln, NE-68588, USA

[2]The University of Texas Rio Grande Valley, Edinburg, TX-78539, USA

Corresponding author: Mircea Chipara, The University of Texas Rio Grande Valley, Department of Physics, 1201 W. University Drive, Edinburg, TX-78539, USA

(E-mail: mircea.chipara@utrgv.edu; chipara@yahoo.com)

## ABSTRACT

Carbon coated nickel nanoparticles dispersed within polystyrene-block polyisoprene-block polystyrene have been investigated by Raman, X-Ray, SQUID, Differential Scanning Calorimetry, and Electron Microscopy. The effect of nanofiller on the self-assembly features of the block copolymer is reported. Preferential localization of nanofiller within the soft phase was noticed below 20 % weight nanofiller. Higher loadings showed uniform distribution of nanofiller within the block copolymer, consistent with the destruction of self-assembly. The effect of nanoparticles' concentration on blocking temperature is discussed.

## KEYWORDS:

Block copolymers; Self-assembly; Squid; DSC; XRD; magnetic properties.

## INTRODUCTION

Recent attention is focused on elastic materials with magnetic features for rheological applications [1], electronics [2], energy [3], data storage [4], and future spintronics [5]. Medical applications [6] are exploiting either the magnetic characteristics for controlled localization and release of drugs or superparamagnetic features for contrast agents in Nuclear Magnetic Resonance Imaging. Block copolymers (BC) such as polystyrene block polyisoprene block polystyrene (PS-bPI-bPS) are attractive matrices, with excellent mechanical properties and rich morphologies derived from their self-assembly capabilities. Dispersion of magnetic nanoparticles (MN) within BC is expected to result in nanocomposites that combine the magnetic characteristics with the elastic features of the matrix [7]. The ability of BC to spontaneously reorganize in ordered structures at submicron scale opens the possibility of new nanomaterials, where the MN are preferentially localized within a given phase of BC [8]. Preliminary data revealed that barium ferrite MN are preferentially trapped within the soft domains (polyisoprene; PI) [7],[8] of PS-bPI-bPS.

Bulk Ni is a ferromagnet with Curie temperature ($T_C$) of 631 K, whose nanoparticle oxidizes easily in air to NiO, an antiferromagnet with a Neel temperature ($T_N$) of 525 K. The blocking temperature, $T_B$, is the temperature at which magnetic properties are averaged out by thermal motions. MNs are characterized by $T_B$ rather than $T_C$ or $T_N$. $T_B$ depends on the size of MN (decreases as the size is decreased) and on the distance between them (due to the competition between dipolar and exchange interactions). Above $T_B$, nanoparticles are superparamagnetic. Typically, MN with spherical morphology (such as Fe, Co, Ni) under 25 nm, are superparamagnetic at room temperature (RT) [9]. The coating with C decreases both the oxidation (by delaying the diffusion of oxygen) and the exchange interactions among MN, allowing for a better dispersion. This justifies the choice of carbon coated Ni nanoparticles (Ni-C) as filler.

## EXPERIMENTAL

PS-bPI-bPS with average degree of polymerization 19,000 containing 17 % polystyrene (PS) was acquired from Sigma-Aldrich. Ni-C, with average size of 20 nm, coated by a 1 nm layer of carbon, was purchased from US Research Nanomaterials, Inc. Solutions of 10 % wt. PS-bPI-bPS in chloroform were prepared and stirred at RT for 1 hour. MNs were dispersed by sonication in chloroform for about 1 h, to enhance their dispersion. Then, these solutions were mixed and

sonicated at 500 W for 1 hour at RT. The as obtained dispersions were poured onto glass slides and the solvent was removed in a vacuum oven at 75 $^{o}$C for 12 hours. Full evaporation was confirmed by TGA measurements in nitrogen. Films containing various amounts of Ni-C in PS-bPI-bPS have been obtained and investigated by Electron Microscopy (Carl Zeiss microscope with EDAX capabilities), X-Ray Diffraction (Bruker Discovery 8 operating in both Wide Angle X-Ray Scattering, WAXS and Small Angle X-Ray Scattering, SAXS modes), Raman Spectroscopy (Bruker Senterra confocal Raman microscope at 785 nm), and Differential Scanning Calorimetry, DSC (Q 200 from TA Instruments). DSC data obtained during the second heating/cooling cycle (at 10 $^{o}$C/min).after a 10 minutes isothermal annealing at 200 $^{o}$C, were recorded. Magnetic properties were investigated by SQUID.

## EXPERIMENTAL RESULTS AND DISCUSSIONS

PS-bPI-bPS has a quasi-continuous phase of PI with spheres or cylinders of PS. Figs. 1A and 1B show the electron microscopy of Ni-C and its elemental composition, respectively. The oxygen's presence reflects the partial oxidation of Ni to NiO. Figs 1C-1G show the nanocomposite containing 10% Ni-C, and its elemental composition (Fig. 1D), indicating well dispersed MN. The distribution of atoms in the sample loaded with 10 % wt. Ni-C is shown in Figs. 1H-1I.

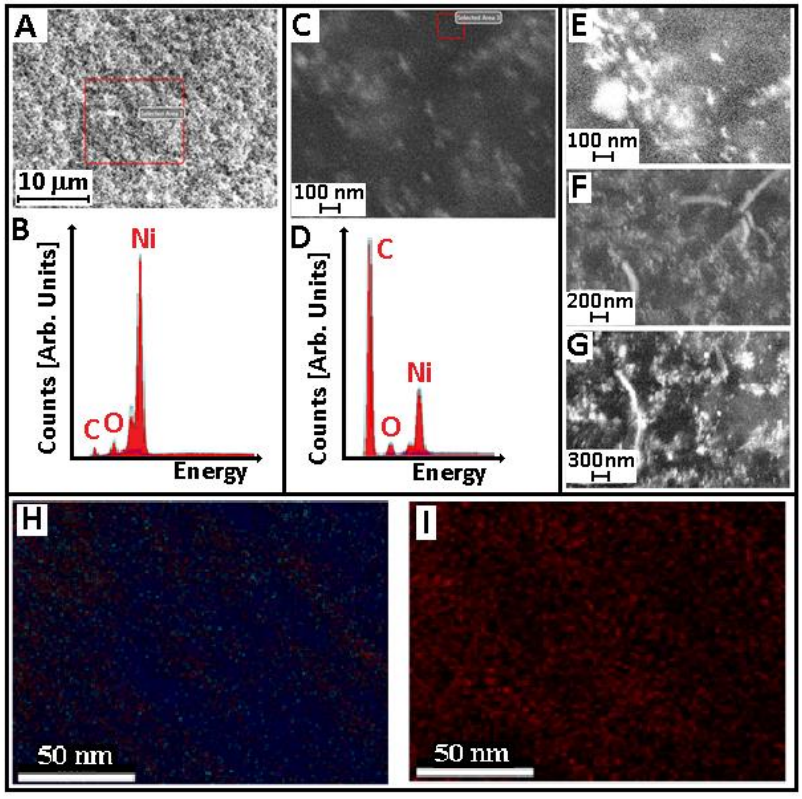


**Fig. 1.** SEM of NiO (**A**) and its elemental composition (**B**). PS-bPI-bPS containing 10% wt. Ni-C (**C**, E, **F**, and **G**) and its elemental composition (**D**). EDAX distribution of atoms (**H, I**) where red is nickel, blue carbon, and cyan oxygen.

Fig. 2 collects the temperature dependence of the magnetization. Pristine Ni-C shows a magnetization (in magnetic field of 100 Oe) of about 3.7 emu/g at 375 K, in

agreement with literature [10]. Field cooled (FC) and zero field cooled (ZFC) magnetization branches have been measured as reported elsewhere [11].

Fig. 2A depicts the temperature dependence of the magnetization for FC and ZFC branches. The splitting between the FC and ZFC branches of the magnetization occurs at the splitting temperature, $T_{DIFF}$, a temperature at which the largest particles are frozen (Fig. 2A) [12], [13]. $T_{DIFF}$ is close to the irreversible temperature $T_{IRR}$, defined by: $[M_{FC}(T_{IRR})-M_{ZFC}(T_{IRR})]/M_{FC}(T_{IRR})<0.01$, where $M_{FC}$ and $M_{ZFC}$ are the sample magnetizations on the FC and ZFC branches, respectively[14]. The dependence of $T_{DIFF}$ on Ni-C concentration is shown in Fig. 2B. $T_{DIFF}$ is almost independent on Ni-C concentration (within the experimental errors), due to the competition between dipolar and exchange interactions as well as to the modification of the volume available to MN within the BC. For a more accurate estimation of $T_B$, the temperature dependence of the magnetization (ZFC branch) was modelled assuming the following additive contributions: a magnetic contribution $A/(T-T_C)$, where $T_C$ is the Curie temperature, a blocking contribution $C/\{1+[(T-T_B)/W]^2\}$represented by a wide Lorentzian of width W centered on $T_B$, and a linear term $D(T-T_A)$, which takes into account the observed quasi-linear dependence of the magnetization on temperature [15]. A, C and D were fitting constants. The best fit was obtained for $A\approx 0$, and $T_C$ oscillating between 0 and -20 K, suggesting weak antiferromagnetic interactions consistent with the oxidation of a thin layer of Ni. $T_B$ was estimated to be in the range 220 to 340 K, in agreement with other experimental data [16].

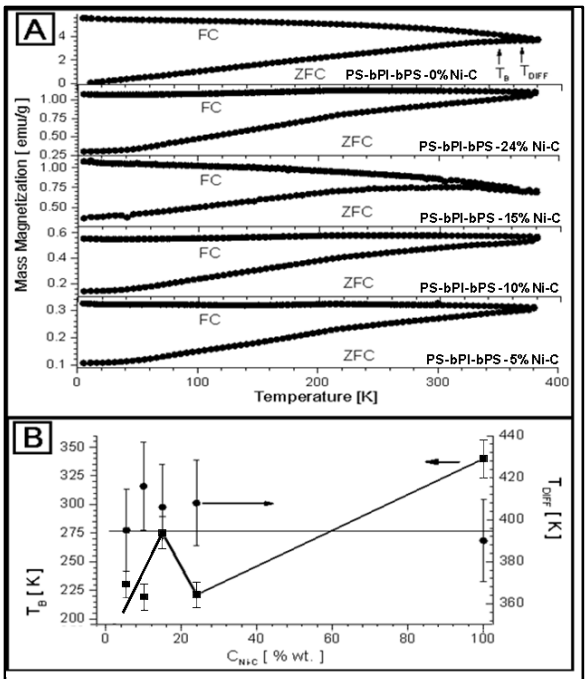


**Fig. 2.** (**A)**.Temperature dependence of magnetization (FC and ZFC) for nanocomposites. (**B)**. Dependence of $T_{DIFF}$ and $T_B$ on Ni-C concentration.

$T_B$ increases as the loading with Ni-C is increased, reflecting the enhancement of dipole and exchange interactions between MN (distance between MN is decreased) [15] (see Fig. 2B). A quasilinear dependence of $T_B$ on the mass fraction of Ni-C is expected [15]. Such a behavior is confirmed by Fig. 2B.However, as the concentration of nanoparticles increases from 10 to 24 %

wt. Ni-C, the magnetization shows a local maxim at about wt. 15 % Ni-C followed by a sudden decrease at about 24 % wt. Ni-C. This indicates that in the concentration range 0 to 20 % wt. Ni-C nanoparticles, the MNs are preferentially located in the soft phase, owing to the segregation between macromolecular chains (self-assembly capabilities of BC). This is consistent with a drop of the distance between MN as their concentration is increased. As the concentration of nanoparticles is increased above 20 % wt, the self-assembly capabilities are destroyed and the whole BC volume becomes available to the MN (i.e. even the polystyrene domains are available to MN). The transition from the localization of MN within the soft phase to the localization of nanoparticles within the whole BC is equivalent to a sudden increase of the average distance between MN, decreasing the contribution of dipole-dipole and exchange interactions.

The Raman spectra of nanocomposites are collected in Fig. 3. The most important lines of cis 1,4 PI are [17] located at 498 (C-C-C deformation), 1001 (C-C stretching), 1375 ($CH_3$ asymmetric deformation), and 1673 (C=C stretching) $cm^{-1}$. Some Raman lines of PS and PI overlap (the most intense PS Raman line located at 1001 $cm^{-1}$ overlaps with the most intense Raman line of PI). However, the line at 2904 $cm^{-1}$ assigned solely to PS, was easily observed and identified. Fig. 3 shows that the Raman lines of PS-bPI-bPS are broadened rapidly by the addition of nanofiller. This is a typical behavior assigned to a dephasing of Raman molecular motions due to the interactions (collisions) between nanofiller and the chains of the polymeric matrix [18].

The carbon coating is extremely disordered contributing to a very weak and broad D band [19], [20] barely visible within the nanocomposites with a high amount of filler. The graphitic band (G-Band) [20] is almost absent.

Fig. 4A collects WAXS data. PS-bPI-bPS spectrum consists of a single broad line, located at $19^o$. No narrow WAXS lines of PS-bPI-bPS are expected at room temperature as the PI component is melted at RT and the PS component is amorphous (atactic). The carbon shell of MNs is expected to show a weak signal at about $21^o$ [21], which probably is masked by the broad line assigned to the polymeric matrix. Fig. 4B shows in more detail the lines due to the face cubic

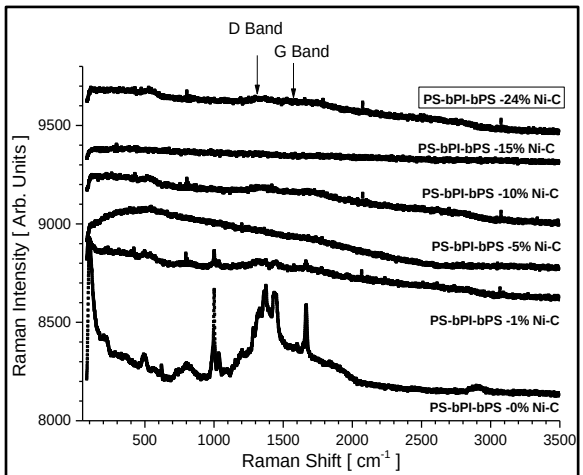


**Fig. 3.** Raman spectra of nanocomposites.

centered Ni nanoparticles, with typical lines at 44°, 52° and 76° assigned to (111), (200) and (220) reflections in Ni [12], [22], [21]. No hexagonal close packed Ni crystallites were observed [23]. The weak line at 75°, was assigned to NiO [24] supporting the Ni-C oxidation. The lines marked with x in Figs 4 originate from the Al substrate. A splitting of all lines assigned to Ni was noticed for doping level above 20 % wt. Ni-C. Tentatively, this splitting was assigned to the filling of both PI and PS domain with Ni-C at high concentration of nanoparticles (due to the destruction of the self-assembly). At low concentration of Ni-C, most nanoparticles are accommodated within the soft PI phase.

Fig. 4C collects the SAXS spectra. It is noticed the presence of a relatively narrow line at very small angles and the shift of the position of this line (accompanied by a drop of the amplitude) towards larger angles as the amount of filler is increased. This spectrum confirms the existence of a statistical order at the nanometer scale, confirming the local self-assembly.

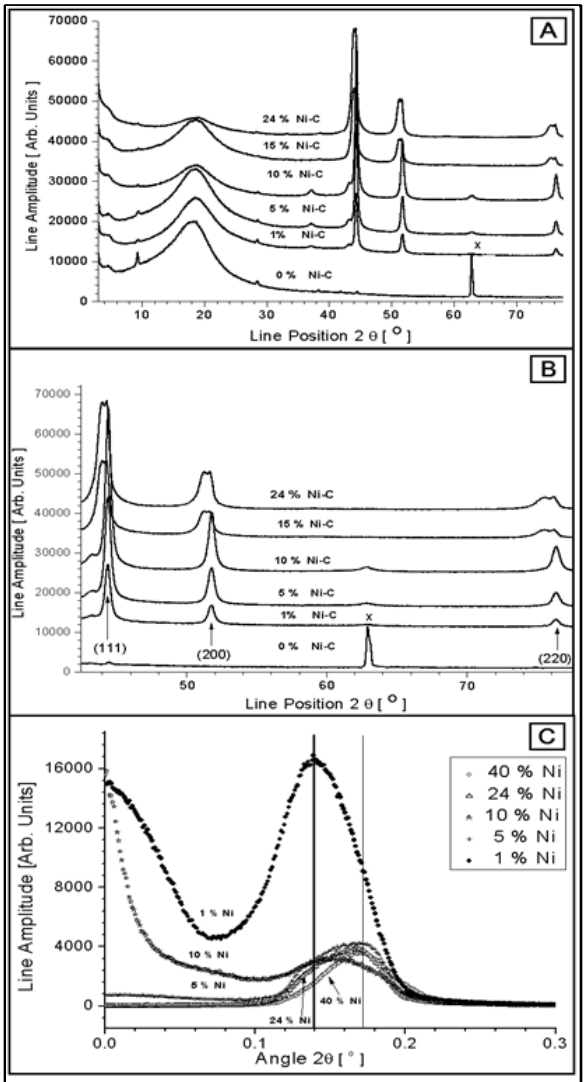


**Fig. 4.** (**A).**WAXS spectra. (**B).** Detailed WAXS lines of Ni-C. (**C).** SAXS spectra.

DSC data provided additional support. As noticed from Fig. 5A, both the pristine polymer and the nanocomposites show no melting/crystallization. A weak glass transition is noticed at 100 °C. This is the typical glass transition temperature ($T_G$) of polystyrene. In the low temperature range, at about -60 °C another $T_G$ assigned to the rubber component (PI) was observed. As expected, the BC is not compatible, showing clear phase separation. More detail is available from Figs. 5B, 5C, where the derivative of the heat exchange with respect to the temperature was represented as a function of temperature. In this representation, the $T_G$ is represented by an extreme (actually the lowest value). It is observed that the $T_G$ of PI decreases as the

concentration of the filler is increased. This indicates an increase of the free volume suggesting a strong stretching of the PI phase due to the addition of the nanofiller. This free volume is generated on the expense of PS available free volume, which is decreased, forcing the $T_G$ of the hard phase (PS) to shift upwards. At high loading with MN this is also the mechanism that destroys the self-assembly of the BC.

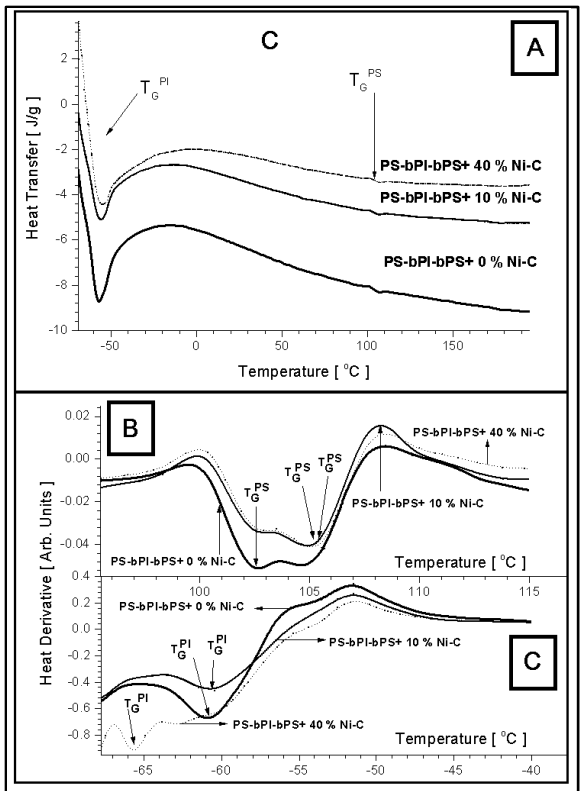


**Fig. 5.** (**A**). DSC thermograms. The derivative of the heat exchange as a function of temperature showing the $T_G$ of PS (**B**) and PI (**C**).

## CONCLUSIONS

The uniform dispersion of Ni-C nanoparticles within PS-bPI-bPS was confirmed. DSC data revealed shifts of $T_G$, for both soft and hard components consistent with the preferential localization of the nanofiller in the soft domains and self-assembly destruction at high loading. Magnetization data indicated that the self-assembly is destroyed at loading in excess of 15 % with Ni-C nanoparticles, in agreement with DSC data. The self-assembly of the polymeric matrix was confirmed by SAXS measurements. Raman spectroscopy confirmed the presence of carbon coatings on Ni-C. X-Ray data were consistent with DSC data, indicating no crystalline component within BC. WAXS data supported the presence of cubic Ni nanoparticles with a small admixture of NiO, consistent with magnetization data.


## ACKNOWLEDGEMENTS.

Research was supported by Nebraska Center for Materials and Nanoscience and acknowledges NSF DMR 1040419 MRI grant "Acquisition of an Environmental Scanning Electron Microscope". UTRGV acknowledges the Department of Defense Grant "Raman Spectrometer for the Characterization of Advanced Materials and Nanomaterials", W911NF-15-1-0063 and the NSF

DMR-1523577: UTRGV-UMN Partnership for Fostering Innovation by Bridging Excellence in Research and Student Success.

**Figure Caption**

**Fig. 1.** SEM of NiO (**A**) and its elemental composition (**B**). PS-bPI-bPS containing 10% wt. Ni-C (**C**, E, **F**, and **G**) and its elemental composition (**D**). EDAX distribution of atoms (**H, I**) where red is nickel, blue carbon, and cyan oxygen.

**Fig. 2. (A).** Temperature dependence of magnetization (FC and ZFC) for nanocomposites. (**B)**. Dependence of $T_{DIFF}$ and $T_B$ on Ni-C concentration.

**Fig. 3.** Raman spectra of nanocomposites.

**Fig. 4.** (**A).**WAXS spectra. (**B).** Detailed WAXS lines of Ni-C. (**C).** SAXS spectra.

**Fig. 5.** (**A).** DSC thermograms. The derivative of the heat exchange as a function of temperature showing the $T_G$ of PS (**B**) and PI (**C**).

**REFERENCES**

[1] K.L. Pickering, S.I. Raa Khim, S. Ilanko, The effect of silane coupling agent on iron sand for use in magnetorheological elastomers part 1: Surface chemical modification and characterization, Compos. Part A Appl. Sci. Manuf. 68 (2015) 377–386.

[2] T. Sekitani, T. Someya, Stretchable, large-area organic electronics., Adv. Mater. 22 (2010) 2228–46.

[3] S. Zhang, Y. Li, L. Peng, Q. Li, S. Chen, K. Hou, Synthesis and characterization of novel waterborne polyurethane nanocomposites with magnetic and electrical properties, Compos. Part A Appl. Sci. Manuf. 66 (2013) 94–101.

[4] K. Xie, B. Wei, Materials and Structures for Stretchable Energy Storage and Conversion Devices., Adv. Mater. 26 (2014) 3592–3617.

[5] S. Sanvito, Organic electronics: Spintronics goes plastic, Nat. Mater. 6 (2007) 803–804.

[6] C. Xu, S. Sun, New forms of superparamagnetic nanoparticles for biomedical applications., Adv. Drug Deliv. Rev. 65 (2013) 732–43.

[7] M. Chipara, R. Skomski, N. Ali, D. Hui, D.J. Sellmyer, Magnetic properties of barium ferrite dispersed within polystyrene-butadiene-styrene block copolymers., J. Nanosci. Nanotechnol. 9 (2009) 3678–3683.

[8] M. Chipara, D. Hui, J. Sankar, D. Leslie-Pelecky, A. Bender, L. Yue, et al., On styrene–butadiene–styrene–barium ferrite nanocomposites, Compos. Part B Eng. 35 (2004) 235–243.

[9] V.R. Galakhov, A. Buling, M. Neumann, N.A. Ovechkina, A.S. Shkvarin, A.S. Semenova, et al., Carbon States in Carbon-Encapsulated Nickel Nanoparticles Studied by Means of X-ray Absorption, Emission, and Photoelectron Spectroscopies, J. Phys. Chem. C. 115 (2011) 24615–24620.

[10] B. Nayak, S. Vitta, A. Nigam, D. Bahadur, Ni and Ni–nickel oxide nanoparticles with different shapes and a core–shell structure, Thin Solid Films. (2006) 9–12.

[11] D. Gozzi, A. Latini, G. Capannelli, F. Canepa, M. Napoletano, M.R. Cimberle, et al., Synthesis and magnetic characterization of Ni nanoparticles and Ni nanoparticles in multiwalled carbon nanotubes, J. Alloys Compd. 419 (2006) 32–39.

[12] W. Li, T. Qiu, L. Wang, S. Ren, J. Zhang, L. He, et al., Preparation and electromagnetic properties of core/shell polystyrene@polypyrrole@nickel composite microspheres., ACS Appl. Mater. Interfaces. 5 (2013) 883–91.

[13] P. Granitzer, K. Rumpf, M. Venkatesan, a. G. Roca, L. Cabrera, M.P. Morales, et al., Magnetic Study of Fe[sub 3]O[sub 4] Nanoparticles Incorporated within Mesoporous Silicon, J. Electrochem. Soc. 157 (2010) K145.

[14] P. Zhang, F. Zuo, F.K.U. Iii, A. Khabari, P. Griffiths, A. Hosseini-Tehrani, Irreversible magnetization in nickel nanoparticles, J. Magn. Ma. 225 (2001) 337–345.

[15] K. Trohidou, M. Vasilakaki, Magnetic Behaviour of Core / Shell Nanoparticle Assemblies : Interparticle Interactions Effects, Acta Phys. Pol. A. 117 (2010) 374–378.

[16] L.M. Moreau, D.-H. Ha, C.R. Bealing, H. Zhang, R.G. Hennig, R.D. Robinson, Unintended phosphorus doping of nickel nanoparticles during synthesis with TOP: a discovery through structural analysis, Nano Lett. 12 (2012) 4530–9.

[17] P. Nallasamy, S. Mohan, Vibrational Spectra of cis-1, 4-polyisoprene, Arab. J. Sci. Eng. 29 (2004) 17–26.

[18] M. Chipara, J.R. Villarreal, M.D. Chipara, K. Lozano, A.C. Chipara, D.J. Sellmyer, Spectroscopic investigations on polypropylene-carbon nanofiber composites. I. Raman and electron spin resonance spectroscopy, J. Polym. Sci. Part B Polym. Phys. 47 (2009) 1644–1652.

[19] K. Bhowmik, A. Mukherjee, M. Mishra, G. De, Stable Ni Nanoparticle–Reduced Graphene Oxide Composites for the Reduction of Highly Toxic Aqueous Cr (VI) at Room Temperature, Langmuir. (2014) 3209–3216.

[20] D.M. Chipara, A.C. Chipara, M. Chipara, Raman Spectroscopy of Carbonaceous Materials : A Concise Review, Spectroscopy. 26 (2011) 2–7.

[21] Y. Huang, Z. Xu, Y. Yang, Preparation, characterization, and surface modification of carbon-encapsulated nickel nanoparticles, J Phys.Chem. C. (2009) 6533–6538.

[22] J. Gong, L.L. Wang, Y. Liu, J.H. Yang, Z.G. Zong, Structural and magnetic properties of hcp and fcc Ni nanoparticles, J. Alloys Compd. 457 (2008) 6–9.

[23] X. Luo, Y. Chen, G.-H. Yue, D.-L. Peng, X. Luo, Preparation of hexagonal close-packed nickel nanoparticles via a thermal decomposition approach using nickel acetate tetrahydrate as a precursor, J. Alloys Compd. 476 (2009) 864–868.

[24] F. Davar, Z. Fereshteh, M. Salavati-Niasari, Nanoparticles Ni and NiO: Synthesis, characterization and magnetic properties, J. Alloys Compd. 476 (2009) 797–801.